

A novel terahertz beam splitter using ultrathin flexible transmission-type coding metasurface

L. LIANG^{a,b,c}, J. WANG^{a,c}, X. YAN^{a,c}, S. GAO^{a,c,*}, Y. LV^{a,c}, L. XIAO^{a,c}, Y. LI^{a,c}, D. WEI^{a,c}, M. WANG^{a,c}, X. WANG^{a,c}, Y. ZHANG^{a,c}, J. YAO^b

^a*School of Opto-electronics Engineering, Zaozhuang University, Zaozhuang 277160, China*

^b*College of Precision Instrument and Opto-electronics Engineering, Tianjin University, Tianjin 300072, China*

^c*Key Laboratory of Optoelectronic Information Processing and Display in Universities of Shandong (Zaozhuang University), Zaozhuang 277160, China*

A new flexible and simple transmission-type coding metasurface was proposed and characterized, which can generate different transmitted beam patterns by coding sequences of “0” and “1” digital elements. The two digital elements with almost identical transmission amplitude are composed of three metallic layers and three dielectric layers, and their transmission phase difference is approximately 180° at 0.95 THz. The characterizations and working mechanisms of the coding metasurface were investigated through theoretical analysis and electromagnetic (EM) simulation. The simulation and theoretical analysis results show that the normally incident waves will be realized a single beam, two main beams and four main beams, respectively using different transmission-type coding sequences. And the amplitude modulation of transmission beam was realized by an optical pump beam. This work reveals a new and simple route for designing novel terahertz beam splitter and offers widespread applications.

(Received December 10, 2018; accepted August 20, 2019)

Keywords: Beam splitter, Coding metasurface, Transmission-type, Digital elements, Coding sequences

1. Introduction

A beam splitter is a function device that can split a beam of light into two or more beams [1-3]. This device has been used for important applications in communication, sensing, light information processing, and imaging [4-9]. Thus, the beam splitter has become a current subject of intense research in microwaves, visible region, and THz wave [10-14]. THz technologies have attracted increasing attention because of strong direction, lower photon energy, fingerprint spectrum, and huge application value in wireless communication, medical diagnosis, aerospace, and other fields [15-22]. Therefore, studying THz beam splitter is a significant task, especially for dynamically tunable beam splitters.

Most of beam splitters were proposed by photonic crystals, semiconductor metasurface, and phase gradient metasurface [23-30]. These ways offer the advantages of low loss, high integration, and high extinction ratio. However the main challenges of these methods are complex fabrication and difficult to free control EM wave. More recently, the reflective coding metasurfaces presented a huge potential for the manipulation of the EM wave, which can achieved anomalous reflection and diffusion, and so on [31-34]. Therefore, the reflective coding metasurfaces provide an effective way for

developing of various functional devices, such as modulators, filters, and polarizer. However, transmission-type coding metasurfaces have been rarely reported, especially in achieving THz beam splitters [35].

In this article, we propose a simple and flexible transmission-type coding metasurface, the coding metasurface is composed of “0” and “1” digital elements, which contain three metallic and three dielectric layers. The two digital elements almost have both the transmission coefficient magnitude and 180° phase difference at about 0.95 THz. They are realized by two different sizes of metallic square ring apertures and circles embedded in multilayer dielectrics. The simulation and theoretical analysis results show that the far-field transmission patterns are changed from a single beam to two, and four beams through the appropriate arrangement of the sequences of “0” and “1” digital elements. When the coding metasurface was covered the layer of semiconductor silicon, the dynamic modulation of beam splitter was achieved under external pump power. Compared with the conventional beam splitter, the proposed beam splitter based on transmission-type coding metasurface has significant features, such as ultrathin structure, easy design and integration.

2. Theoretical analysis

The transmission of single beam with any incident

EM plane wave will be split two or more beams by designing an ultrathin and flexible transmission-type coding metasurface, as shown in Fig. 1(a).

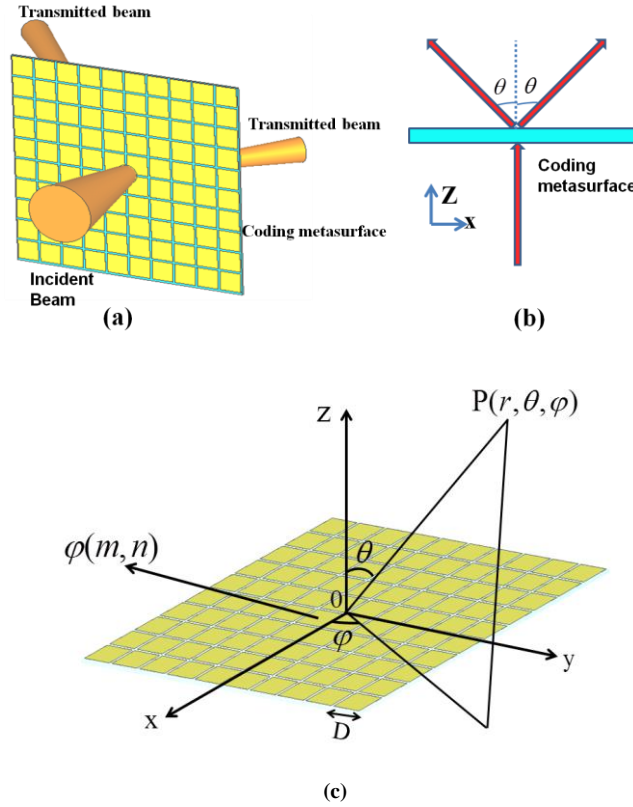


Fig. 1. (a) Schematic of proposed beam splitter by transmission-type coding metasurface (b) Top view of beam splitter by transmission-type coding metasurface (c) Schematic of coding metasurface, which contains $N \times N$ equal-size lattice with dimension D ; each lattice is occupied by “1” or “0” digital elements

Fig. 1(b) shows the top view of the beam splitter using the coding metasurface. The proposed transmission-type coding metasurface is presented in Fig. 1(c), which is composed of $N \times N$ equal-sized array with

dimension D . “1” or “0” digital elements occupy of each square lattice.

The far-field radiated function through the coding metasurface can be expressed as [31]:

$$f(\theta, \varphi) = f_e(\theta, \varphi) \sum_{m=1}^N \sum_{n=1}^N \exp \left\{ -i \left[\varphi(m, n) + KD \sin \theta \left(m - \frac{1}{2} \right) + \left(n - \frac{1}{2} \right) \sin \varphi \right] \right\} \quad (1)$$

where $f_e(\theta, \varphi)$ is the far radiation pattern function of a square lattice. The scattering phase of the mn -th lattice is assumed to be $\varphi(m, n)$, which is either 0° or 180° . And θ and φ are the elevation and azimuth angles,

respectively.

The directivity function $Dir(\theta, \varphi)$ of the metasurface can be given as:

$$Dir(\theta, \varphi) = 4\pi \frac{|f(\theta, \varphi)|^2}{\int_0^{2\pi} \int_0^\pi |f(\theta, \varphi)|^2 \sin \theta d\theta d\varphi} \quad (2)$$

The $f_e(\theta, \varphi)$ term is eliminated because of the 180°

phase difference between “0” and “1” digital elements.

By treating each of the two digital elements as a dipole radiation source, the far-field radiation of the transmission can be explained by the interference and superposition principle of the electromagnetic wave for two digital elements. The transmission coefficient of the two digital elements in the design process have the same amplitude, but the transmission phase difference is approximately 180° between “1” and “0” at a certain frequency or over a frequency band. Therefore, the $f_e(\theta, \varphi)$ term has been eliminated because of the destructive interference between two digital elements, and the transmitted far-field patterns can be achieved through different coding sequences of the metasurface.

3. Design of the coding metasurface and discussion

Compared with the conventional beam splitter, the design of the ultrathin beam splitter based on the coding metasurface faces challenges in terms of the phase profile and transmission efficient. We proposed a triple-layered metallic metasurface to achieve these requirements, as shown in Fig. 2(a).

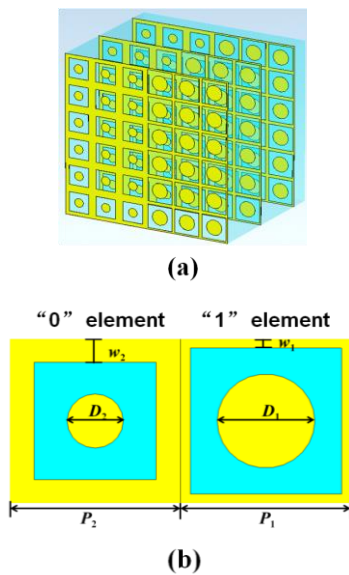


Fig. 2. (a) Schematic of the transmission-type coding metasurface that consist of three metallic layers and three polyimide spacers (b) Configuration of “0” and “1” elements and their dimensions are $P_1=P_2=140 \mu\text{m}$, $w_1=8 \mu\text{m}$, $w_2=20 \mu\text{m}$, $D_1=80 \mu\text{m}$, $D_2=46 \mu\text{m}$, respectively

Each metallic structure layer is separated by a polyimide spacer with $30 \mu\text{m}$ thickness, and the bottom metallic layers are intentionally insulated with a $5 \mu\text{m}$ -thick polyimide layer for easy processing. The permittivity and loss tangent of polyimide are 3.1 and

0.05, respectively. The metallic structure layer is composed of a square ring aperture and a circle with two different geometric parameters, as shown in Fig.2 (b). The lattice period is $P_1=P_2=140 \mu\text{m}$, the width for a square ring aperture is $w_1=8 \mu\text{m}$, $w_2=20 \mu\text{m}$, and the diameter of the circle is $D_2=46 \mu\text{m}$, $D_1=80 \mu\text{m}$, respectively.

To characterize the proposed coding metasurface, we simulated the magnitude and phase of the transmission as a function of frequency for the different metallic structures united by CST Microwave Studio, as shown in Fig. 3. The plane wave is normally incident to the periodically arranged unit cells along the z-axis, the electric field and magnetic field are applied along the x and y directions.

The simulation results show that the transmission amplitude over 0.5 is achieved over a frequency range from 0.70 THz to 0.99 THz, and is equal to the transmission amplitude at 0.95 THz of this type of metallic structure. The transmission phase difference is about 180° at 0.95 THz. We define the “0” and “1” digital elements for two different sizes of metallic structures because their calculated phase difference is about 180° at 0.95 THz. The proposed metasurface is a coding metasurface with “0” and “1” digital elements, and the proposed beam splitter is designed to work at 0.95 THz using this transmission-type coding metasurface.

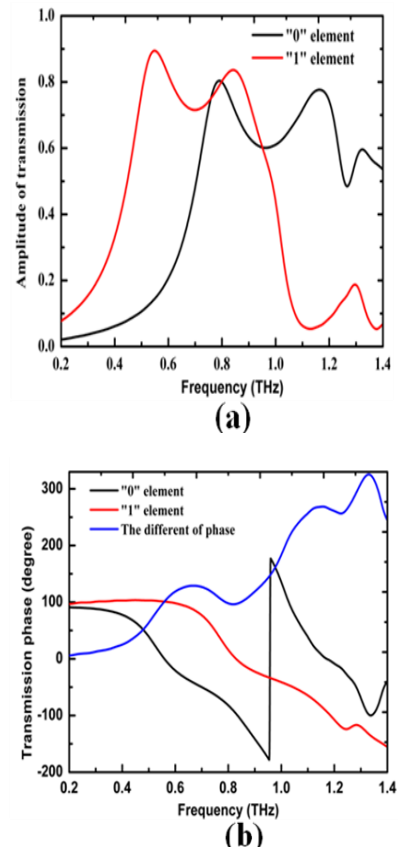


Fig. 3. (a) Simulated transmission amplitude of “0” and “1” digital elements (b) Simulated transmission-phase and their difference phase of “0” and “1” digital elements

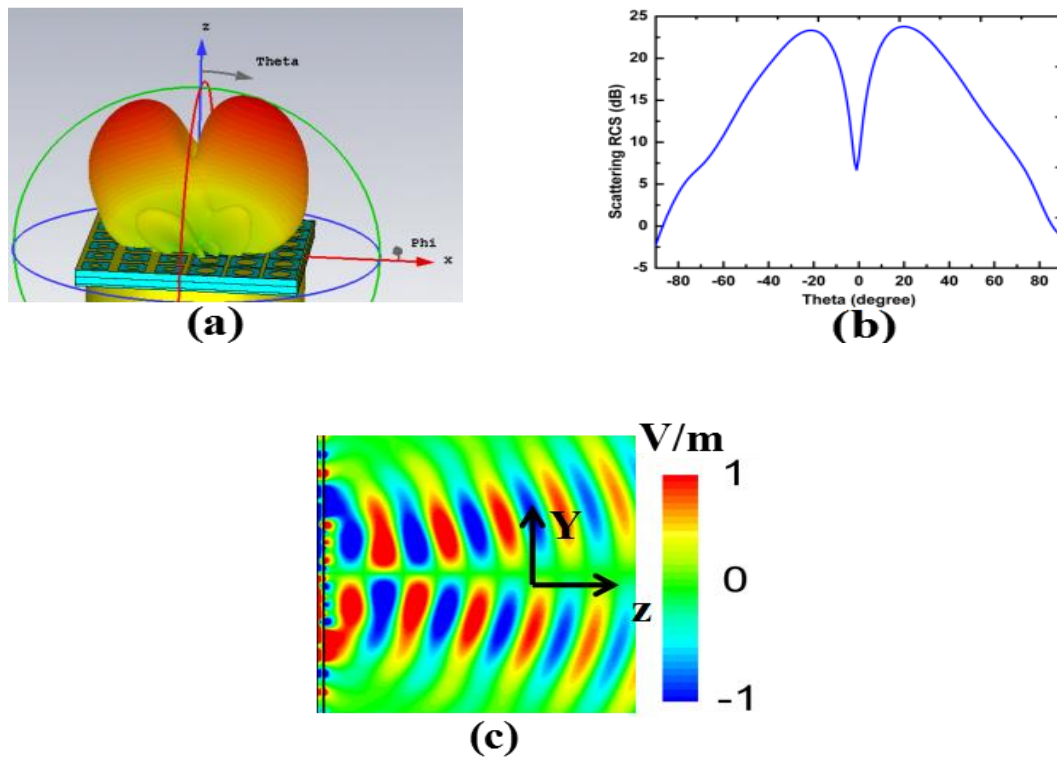


Fig. 4. (a) Simulated 3D field patterns of the coding metasurface under the normal incidence at 0.95 THz (b) Simulated 2D far-field patterns in the XOZ plane of the coding metasurface (c) Near electric field distribution of the effect on the YOZ plane at 0.95 THz

First, we evaluate the properties of the proposed coding metasurface by simulating the far-field patterns and near-field distributions at 0.95 THz, as shown in Fig. 4. Fig. 4(a) show that the 3D field patterns of coding metasurface with periodic sequence of 000111.../000111..., the results show that the two anomalous direction beams of the transmission. And each of transmission peaks can be clearly observed at $\pm 20^\circ$ in the x-z plane of Fig. 4(b). This phenomenon can be further verified by the near-field patterns at 0.95 THz, as shown in Fig. 4(c). When the incident wave is impinging normally to the surface of the transmission-type coding metasurface, the incident wave are transmitted into two different directions with the angles of -20° and $+20^\circ$, respectively.

To further achieve the different functions of the splitter beam, we studied the transmission-type coding metasurface with different coding sequences of “0” and “1” elements, as shown in Figs. 5(a-c). The simulation results show that the normally incident beam will be transmitted as a single main beam for the periodic coding sequence of 000000.../000000..., as shown in Fig. 5(d). Under the periodic coding sequence of 000111.../000111...and 000111.../111000... for the coding metasurface, the normally incident of single beam will be transmitted as two or four main beams in symmetrically oriented directions, respectively, as illustrated in Fig. 5 e and f. The aforementioned simulation results show that the designed transmission-type coding metasurfaces can control far field transmission patterns by different coding sequences under the normal incidence of EM waves.

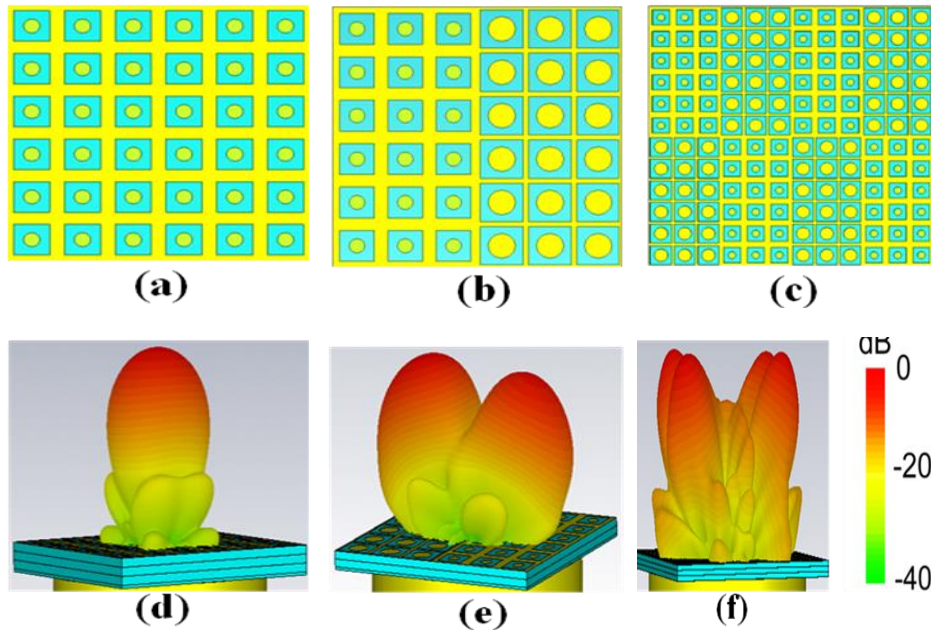


Fig. 5. (a–c) Transmission-type coding metasurface with different sequences: (a) 000000.../000000..., (b) 000111.../000111... (c) 000111.../111000... (d–f) Simulation results of the coding metasurfaces with different coding sequences: (d) a single main transmission beam (e) two main beams, and (f) four main beams

In order to broaden the application rang of designed beam splitter, we further studied the dynamic control characteristics of this devices. Fig. 6. (a) show the schematic of optically controlled terahertz coding metasurface, it is covered the photoconductive semiconductors silicon with thickness 300 nm. The permittivity of silicon is 11.68, but the conductivity silicon is a change value according to different pump light powers [36].

The characteristics of transmission beams for

000111.../000111...periodic sequence of coding metasurface were simulated for silicon with different conductivity at 0.95THz, as shown in Fig. 6(b–d). From the simulation results as shown in Fig. 6, the amplitude of transmission beams can be modulated when the silicon conductivity ranges from $\sigma = 1s/m$ to $\sigma = 3 \times 10^4 s/m$. This is because that the silicon can be changed from dielectric to metal when increasing the conductivity of the silicon layer, leading to different and transmission coefficients of the beams for coding metasurface.

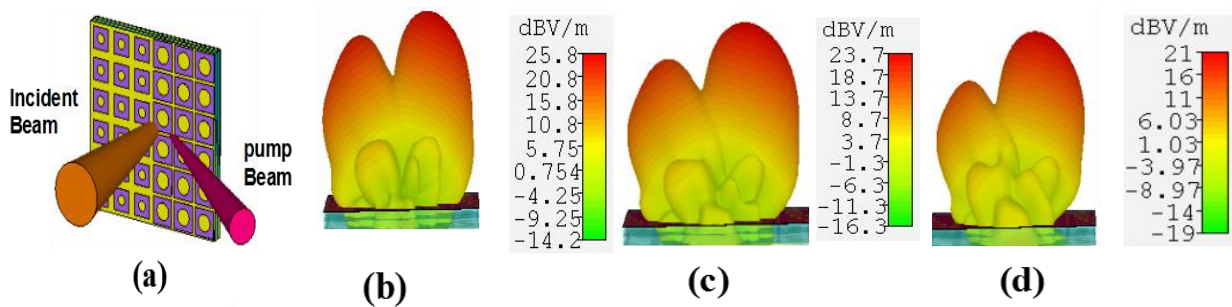


Fig. 6. (a) Schematic of optically controlled terahertz coding metasurface (b–d) The transmission two beams of 000111.../000111...coding metasurface for silicon with different conductivity at 0.95THz (b) $\sigma = 1s/m$ (c) $\sigma = 1 \times 10^4 s/m$ (d) $\sigma = 3 \times 10^4 s/m$

The simulation results can be explained by the following theories [31]:

(1) Under the periodic transmission-type coding sequence of 000000.../000000..., the Eq. (1) can be expressed as:

$$|f_1(\theta, \varphi)| = C_1 |\cos \psi_1 + \cos \psi_2| = 2C_1 \left| \cos \frac{\psi_1 + \psi_2}{2} \cos \frac{\psi_1 - \psi_2}{2} \right| \quad (3)$$

where

$$\begin{aligned}\psi_1 &= \frac{3}{2}KD(\sin\theta\cos\varphi + \sin\theta\sin\phi), \\ \psi_2 &= \frac{3}{2}KD(-\sin\theta\cos\varphi + \sin\theta\sin\phi)\end{aligned}\quad (4)$$

$$\left|\cos\frac{\psi_1+\psi_2}{2}\right|=1, \left|\cos\frac{\psi_1-\psi_2}{2}\right|=1 \quad (5)$$

From Eqs.(4) and (5), we can obtain $\theta_1=0$ and generate a main transmission beam direction to the axis of coding metasurface, which is consistent with the simulation results.

(2) For the 000111.../000111... transmission-type coding sequence metasurface, the Eq. (1) can be expressed as:

$$|f_2(\theta, \varphi)| = C_2 |\sin\psi_1 + \sin\psi_2| = 2C_2 \left| \sin\frac{\psi_1+\psi_2}{2} \cos\frac{\psi_1-\psi_2}{2} \right| \quad (6)$$

$$\left|\sin\frac{\psi_1+\psi_2}{2}\right|=1, \left|\cos\frac{\psi_1-\psi_2}{2}\right|=1 \quad (7)$$

From Eqs. (6) and (7), we can derive that $\varphi_2=90^\circ$ and 270° , and $\theta_2 = \arcsin\frac{\lambda}{2*3D}$. Thus, this coding sequence metasurface can generate two main transmission beams direction to the $(\theta_2, 90^\circ)$ and $(\theta_2, 270^\circ)$.

The preceding theoretical analysis, show that the angle $\theta=20.92^\circ$ has a good agreement with the simulation result ($\theta=20^\circ$) for this proposed coding transmission-type metasurface.

(3) For the 000111.../111000... transmission-type coding sequence metasurface, the Eq. (1) can be expressed as:

$$|f_3(\theta, \varphi)| = C_3 |\cos\psi_1 - \cos\psi_2| = 2C_3 \left| \sin\frac{\psi_1+\psi_2}{2} \sin\frac{\psi_1-\psi_2}{2} \right| \quad (8)$$

$$\left|\sin\frac{\psi_1+\psi_2}{2}\right|=1, \left|\sin\frac{\psi_1-\psi_2}{2}\right|=1 \quad (9)$$

We derive that $\varphi_3=45^\circ, 135^\circ, 225^\circ, 315^\circ$, and $\theta_3 = \arcsin\frac{\lambda}{\sqrt{2}*3D}$, which imply four transmission beams for this coding sequence of the metasurface.

Therefore, different direction transmission beams can be controlled by different coding sequences of metasurface. And diverse types beam splitters will be achieved through using transmission-type coding metasurface.

4. Conclusion

We proposed and analyzed a novel ultra-thin transmission-type coding metasurface based on two digital elements, which can generate different transmitted beams. The two digital elements have three metallic layers and dielectric layers; which exhibit almost identical transmission amplitude and 180° for transmission phase difference at 0.95 THz. Numerical results and theoretical analysis show that a single main beam, two main beams, and four main beams can be achieved by different transmission-type coding sequences. The amplitude of transmission beams can be

tuned by increasing the conductivity of the silicon layer. The proposed approach provides a new technology for designing THz beam splitter, which possesses great application values in communication, sensing, imaging, etc.

Acknowledgements

This work was supported by the National Natural Science Foundation of China (Grant numbers 61701434, 61735010 and 61675147); the Natural Science Foundation of Shandong Province (Grant numbers ZR2017MF005, ZR2018LF001); The National Key Research and Development Program of China (Grant numbers 2017YFB1401203, 2017YFA0700202); the China Postdoctoral Science Foundation (Grant number 2015M571263); the Programme of Independent and Achievement Transformation plan for Zaozhuang (Grant numbers 2016GH19, 2016GH31); Zaozhuang Engineering Research Center of Terahertz; the Project Special Funding of Taishan Scholar.

References

- [1] T. Niu, W. Withayachumnankul, A. Upadhyay, P. Gutruf, D. Abbott, M. Bhaskaran, C. Fumeaux, *Opt. Express* **22**, 16148 (2018).
- [2] B. S.-Y. Ung, B. Weng, R. L. Shepherd, D. Abbott, C. Fumeaux, *Opt. Mater. Express* **3**, 1242 (2013).
- [3] F. Defrance, M. Casaletti, J. Sarrazin, M. C. Wiedner, H. Gibson, G. Gay, R. Lefèvre, *Opt. Express* **24**, 20335 (2016).
- [4] X. W. Guan, H. Wu, Y. C. Shi, and D. X. Dai, *Opt. Lett.* **39**, 259 (2016).
- [5] B. I. Akkca, B. Považay, A. Alex, K. Wörhoff, R. M. de Ridder, W. Drexler, *Opt. Express* **21**, 16648 (2013).
- [6] J. Wang, D. Liang, Y. B. Tang, D. X. Dai, J. E. Bowers, *Opt. Lett.* **38**, 4 (2013).
- [7] D. X. Dai, Z. Wang, J. Peters, J. E. Bowers, *IEEE Photon. Tech. Lett.* **24**, 673 (2015).
- [8] B. Wang, L. Chen, L. Lei, J. Y. Zhou, *IEEE Photon. Tech. Lett.* **25**, 863 (2013).
- [9] N. Prtljaga, R. J. Coles, J. O'Hara, B. Royall, A. M. Fox, E. Clarke, M. S. Skolnick, *Appl. Phys. Lett.* **104**, 231107 (2014).
- [10] J. Hammer, S. Thomas, P. Weber, P. Hommelhoff, *Phys. Rev. Lett.* **114**, 254801 (2015).
- [11] G. L. Gattobigio, A. Couvert, G. Reinaudi, B. Georgeot, D. Guéry-Odelin, *Phys. Rev. Lett.* **109**, 030403 (2012).
- [12] A. Cottet, *Phys. Rev. B* **86**, 075107 (2012).
- [13] S. Li, H. Zhang, Y. Hou, J. J. Bai, W. W. Liu, S. J. Chang, *Appl. Optics* **52**, 3305 (2013).
- [14] Z. X. Su, X. Chen, J. B. Yin, X. P. Zhao, *Opt. Lett.* **41**, 3799 (2016).
- [15] M. Tonouchi, *Nat. Photonics* **1**, 97 (2007).
- [16] J. S. Melinger, S. S. Harsha, N. Laman, D. Grischkowsky, *Opt. Express* **18**, 27238 (2010).
- [17] P. U. Jepsen, D. G. Cooke, M. Koch, *Laser & Photonics Reviews* **5**, 124 (2011).
- [18] H.-J. Song, T. Nagatsuma, *IEEE Tran. Terahertz Science and Technology* **1**, 256 (2011).
- [19] E. Arik, H. K. Altan, O. Esenturk, *J. Phys. Chem. A* **118**, 3081 (2014).
- [20] R. Fukasawa, *IEEE Trans. THz Sci. Technol.* **5**, 1121 (2015).
- [21] X. Yang, K. Yang, Y. Luo, W. L. Fu, *Appl. Microbiol. Biot.* **100**, 5289 (2016).
- [22] I. M. Saied, M. Meribout, E. Kato, X. H. Zhao, *IEEE Tran. Terahertz Science and Technology* **7**, 250 (2017).
- [23] J. H. Lee, J. W. Yoon, M. J. Jung, J. K. Hong, S. H. Song, R. Magnusson, *Appl. Phys. Lett.* **104**, 233505 (2016).
- [24] M. D. Turner, M. Saba, Q. M. Zhang, B. P. Cumming, G. E. Schröder-Turk, M. Gu, *Nature Photonics* **7**, 801 (2013).
- [25] G. Q. Mo, J. S. Li, *Appl. Optics* **55**, 7093 (2016).
- [26] X. Liu, D. X. Yang, *Chin. Phys. B* **25**, 047301 (2016).
- [27] W. L. Guo, G. M. Wang, S. S. Ding, H. P. Li, T. Cai, *Chin. Phys. B* **25**, 084101 (2016).
- [28] W. Y. Zhao, H. Jiang, B. Y. Li, J. Song, Y. Y. Jiang, *Appl. Phys. Lett.* **108**, 181102 (2016).
- [29] J. S. Li, H. Li, L. Zhang, *Appl. Optics* **53**, 5024 (2014).
- [30] S. L. Jia, X. Wan, D. Bao, Y. J. Zhao, T. J. Cui, *Laser Photonics Rev.* **9**, 545 (2015).
- [31] T. J. Cui, M. Q. Qi, X. Wan, J. Zhao, Q. Cheng, *Light: Science and Applications* **3**, e218 (2014).
- [32] H. Tao, M. A. Brenckle, M. M. Yang, J. D. Zhang, M. K. Liu, S. M. Siebert, R. D. Averitt, M. S. Mannoer, M. C. McAlpine, J. A. Rogers, D. L. Kaplan, F. G. Omenetto, *Adv. Opt. Mater.* **24**, 1374 (2015).
- [33] S. Liu, T. J. Cui, Q. Xu, D. Bao, L. L. Du, X. Wan, W. X. Tang, C. M. Ouyang, X. Y. Zhou, H. Yuan, H. F. Ma, W. X. Jiang, J. G. Han, W. L. Zhang, Q. Cheng, *Light: Science and Applications* **5**, e16076 (2016).
- [34] X. Wan, M. Q. Qi, T. Y. Chen, T. J. Cui, *Sci. Rep.* **6**, 20663 (2016).
- [35] Y. B. L, L. L. Li, B. B. Xu, W. Wu, R. Y. Wu, X. Wan, Q. Cheng, T. J. Cui, *Sci. Rep.* **6**, 23731 (2016).
- [36] V. R. Almeida, C. A. Barrios, R. R. Panepucci, M. Lipson, *Nature* **431**, 1081 (2004).

*Corresponding author: gaoshan12260 @126.com